



LAWRENCE
LIVERMORE
NATIONAL
LABORATORY

Divertor with a Third-Order Null of the Poloidal Field

D. D. Ryutov, M. V. Umansky

June 6, 2013

The Physics of Plasmas

Disclaimer

This document was prepared as an account of work sponsored by an agency of the United States government. Neither the United States government nor Lawrence Livermore National Security, LLC, nor any of their employees makes any warranty, expressed or implied, or assumes any legal liability or responsibility for the accuracy, completeness, or usefulness of any information, apparatus, product, or process disclosed, or represents that its use would not infringe privately owned rights. Reference herein to any specific commercial product, process, or service by trade name, trademark, manufacturer, or otherwise does not necessarily constitute or imply its endorsement, recommendation, or favoring by the United States government or Lawrence Livermore National Security, LLC. The views and opinions of authors expressed herein do not necessarily state or reflect those of the United States government or Lawrence Livermore National Security, LLC, and shall not be used for advertising or product endorsement purposes.

Divertor with a third-order null of the poloidal field

D.D. Ryutov, M.V. Umansky

Lawrence Livermore National Laboratory, Livermore, CA 94551, USA

Abstract

A concept and preliminary feasibility analysis of a divertor with the third-order poloidal field null is presented. The third-order null is the point where not only the field itself but also its first and second spatial derivatives are zero. In this case, the separatrix near the null-point has eight branches, and the number of strike-points increases from 2 (as in the standard divertor) to six. It is shown that this magnetic configuration can be created by a proper adjustment of the currents in a set of divertor coils situated at a significant distance from the null. If the currents are somewhat different from the required values, the configuration becomes that of three closely-spaced first-order nulls. Analytic approach, suitable for a quick orientation in the problem is used. Potential advantages and disadvantages of this configuration are briefly discussed.

Recently a divertor where the poloidal field null is close to the second-order null has drawn some attention both in theory (e.g., [1, 2]) and experiment (e.g., [3-5]). The second-order null means that not only the poloidal field (PF) but also its first spatial derivatives turn zero at the same point [1]. Alternatively, one can say, that the second-order null is formed as a result of merging of two first-order nulls [6, 7].

The second-order null leads to a formation of the separatrix with six branches instead of the four branches as in the first-order null. The number of the strike-points increases from two to four. The poloidal field strength B_p near the second-order null scales as r^2 with the distance r from the null, compared to the linear dependence, $B_p \sim r$, for the first-order null. This leads to significant changes of the field structure not only on the open but also on the closed field lines. In particular, the safety factor and the magnetic shear inside the separatrix increase significantly

on the closed flux surfaces near the separatrix [1, 2]. Another related change is a significant increase of the prompt ion loss from the area just inside the separatrix [8].

Other interesting concepts for improving the performance of the divertors are represented by the concepts of an X-divertor [9, 10] and the super-X divertor [11]. In the first of them, additional dipole coils are used in the divertor legs of a standard X-point divertor to create a significant poloidal field reduction near the strike points – see, e.g., Fig. 1d of Ref. [10]. In the second one, the outer divertor “leg” is stretched (by means of additional PF coils) to a larger major radius R , to exploit the proportionality of the wetted surface area to R . One can additionally expand the fluxtube near the strike point in the same way as in an X-divertor.

The present article is based on the same general idea as a snowflake configuration, but extends it to the situation of the next, third-order, PF null or to an approximate third-order null. We demonstrate that this can be done with a reasonable set of coils. The potential benefits include an easier onset of the convection around the PF null discussed in Refs. [12] and [13], and an appearance of additional strike points. As with the snowflake, maintaining an exact third-order null is impossible, since in the parameter space (made of the plasma and PF coil currents) it lies on the zero-measure manifold, so that a small change of the currents in the coils or in the plasma would lead to the splitting of the third-order nulls to three first-order nulls. On the other hand, if the nulls are situated at a small distance from each other, the situation for the external observer does not differ from an exact one (similarly to the snowflake).

For the distance r from the third-order null (or from the three narrowly-spaced first-order nulls) small compared the major radius R , $r \ll R$, the effects of the toroidal curvature are small (Cf. [1], [7]) and one can consider a planar (x,y) geometry (Fig. 1). We will describe the magnetic field by the flux-function $V(x,y)$ such that $B_x = \partial V / \partial y$; $B_y = -\partial V / \partial x$. Assuming that

the currents in the divertor zone are negligibly small, so that $\nabla \times \mathbf{B} = 0$, we find that V satisfies the Laplace equation, $\nabla^2 V = 0$. If we reach an exact third-order null, the flux function should scale as r^4 . Then, if one substitutes this dependence into the Laplace equation, $(1/r)\partial(r\partial V/\partial r) + (1/r^2)(\partial^2 V/\partial \varphi^2) = 0$, one finds that the dependence on the azimuthal angle φ is $\cos 4(\varphi - \varphi_0)$, so that $V = \text{const} \cdot r^4 \cos 4(\varphi - \varphi_0)$ (we omit an arbitrary additive constant). The angle φ_0 characterizes the orientation of the branches of the separatrix. Obviously, for the just described flux function the magnetic field strength $|\mathbf{B}_p| = \sqrt{B_r^2 + B_\varphi^2} = 4\text{const} \cdot r^3$ does not depend on the angle φ , it depends only on r .

We assess the general reasonableness of the constraints on the PF coil location in the simple model where the plasma is approximated by a single-wire current situated at the distance a from the desired null, whereas the divertor coils would be described by three wire system (Fig.1). Compared to the snowflake, where the second-order null in the similar configuration could be created by two divertor currents, we need here three currents, because of an additional constraint on the field is imposed (zero second derivative of B_p). We start from assessing an “exact” 3rd order null geometry and then move on to describe the deviations from it.

The problem contains a number of input parameters: the plasma current I_p , the current I_l in each of the two horizontally-shifted coils, and current I_2 in the vertically-shifted coil; in addition, we have four geometrical parameters, a , b , c , and d (Fig. 1).

For the symmetry reason, the separatrix branches in the configuration of Fig. 1 will be symmetric with respect to the vertical axis. Note the sign convention described in a figure caption. Obviously, in order for a PF coil not to be inside the confined plasma, the parameter c should be positive. The parameter b is positive when the pair of the horizontally-spaced coils is

situated below the null. The parameters d and a are also positive. In what follows, we normalize the currents $I_{1,2}$ to the plasma current I_p , and the parameters b , c and d to the distance a . Still, we have five input parameters: two normalized currents and three normalized distances, and this seems to make the problem not quite amenable to the analytic approach that we pursue here. However, as has been mentioned above, the field strength $|\mathbf{B}_p|$ does not depend on the direction. This allows us to consider the radial dependence of the x -component only along the y axis. There is no need to find all the numerous cross derivatives to guarantee that the field indeed scales properly.

So, we impose the following three constraints at $x = y = 0$: $B_x = 0$; $\partial B_x / \partial y = 0$; $\partial^2 B_x / \partial y^2 = 0$. For the configuration of Fig. 1, the field strength on the vertical axis is (in the CGS units that we use throughout the paper):

$$B_x(y) = \frac{2}{c} \left[\frac{I}{a-y} - \frac{2I_1(b+y)}{\frac{d^2}{4} + (b+y)^2} - \frac{I_2}{c+y} \right] \quad (1)$$

Thus far we have been using the dimensional quantities. Imposing the aforementioned constraints on the field strength and its derivatives at $y=0$, we find three equations relating the five dimensionless parameters. By choosing two of them, specifically b and d , as input parameters, we find, after some algebra, the other three parameters (now in the normalized units):

$$c = \frac{b \left(b^2 + \frac{d^2}{4} \right)^2 + \left(b^4 - \frac{d^4}{16} \right)}{b \left(b^2 - \frac{3d^2}{4} \right) + \left(b^4 - \frac{d^4}{16} \right)} \quad (2)$$

$$I_1 = \frac{(1+c)\left(b^2 + \frac{d^2}{4}\right)^2}{2b\left(b^2 + \frac{d^2}{4}\right) - 2c\left(b^2 - \frac{d^2}{4}\right)} \quad (3)$$

$$I_2 = c \left[1 - \frac{2bI_1}{b^2 + \frac{d^2}{4}} \right] \quad (4)$$

Examples of the flux surfaces for $d=0.5$ are presented in Fig. 2 for several values of b . The corresponding values of the divertor coil currents are shown in Table 1. What is remarkable here is that the coils can be situated quite far from the divertor null and that the divertor currents are relatively moderate. For a tokamak with $a \sim 7$ m, one could have $d \sim 3.5$ m, $c \sim 1.5$ m. One has of course to remember that the magnetic configuration depicted in Fig. 1 does not provide a correct magnetohydrodynamic (MHD) equilibrium (as most of the few-wire models). In the context of the snowflake divertor this point was correctly made by Lackner and Zohm [14]. So, our discussion here just illustrates the possible structure of the magnetic field in the divertor area and the sensitivity of the configuration to possible inaccuracies in the values of the currents.

The shape of the separatrix shown in Fig. 3, with one main “petal” and three divertor “petals” resembles a four-petal cloverleaf, which we will use further for designation of the configuration.

Obviously, in the cloverleaf divertor there are six strike points that can be used for collecting the heat flux, compared to four in the snowflake divertor and two in the standard divertor. It is also obvious that the flux expansion near the null is stronger than in either standard or snowflake divertor. The plasma safety factor q on the closed flux surfaces inside the separatrix becomes much higher: it diverges as $|\delta V|^{-1/2}$ where δV is the poloidal flux minus the flux at the

separatrix, compared to $\ln|\delta V|^{-1}$ and $|\delta V|^{-1/3}$ for the standard null and the snowflake divertor. The magnetic shear just inside the separatrix also becomes much higher. The connection length on the open flux surfaces increases significantly, as does the volume of the SOL plasma near the null.

An important parameter that characterizes the size of the zone of a low poloidal field near the null-point is a coefficient in the expression $B_p = \text{const} \cdot r^3$ in the vicinity of the null. The radius r will be normalized to the minor plasma radius for which we will use a rough estimate of $a/2$. It is convenient to normalize the field near the null to the poloidal field at the last closed flux surface at the midplane, B_{pm} . As a characteristic value for it we use $B_{pm} = 2I_p/c(a/2)$. In other words, we represent the field near the null in the form

$$B_p = K(2r/a)^3 B_{pm}, \quad (5)$$

where K is a dimensionless coefficient. It can be found by taking the third derivative of Eq. (1) at $y=0$ and substituting into it the values of c , I_1 and I_2 from Eqs. (2)-(4). This dimensionless coefficient will depend only on the normalized values of b and d . By taking the third derivative of Eq. (1), one finds the following expression for K in terms of our basic parameters b and d :

$$K = \frac{1}{16} \left| 1 + I_1 \frac{2b^4 - 3b^2d^2 + \frac{d^4}{8}}{\left(b^2 + \frac{d^2}{4}\right)^4} + \frac{I_2}{c^4} \right| \quad (6)$$

where c , I_1 and I_2 are defined by Eqs. (2)-(4), and b and d are normalized to a . The values of coefficient K for several basic parameters b and d are presented in Table 1.

Consider as a reference the case of $d/a=0.5$ and $b/a=0.1$. For it, $K=8.96$. According to Eq. (5), it means that the magnetic field will be 30 times less than B_{pm} in a volume of a radius $r \sim 0.08a$ around the null. For a facility with $a \sim 7\text{m}$ one would have $d \sim 3.5\text{ m}$ and $c \sim 1.4\text{ m}$ the

field will be that low for $r < 55$ cm. The importance of this low- B_p zone has been highlighted in Refs. [12, 13] in conjunction with the mechanism of convective spreading of the plasma flow over all the divertor legs and widening of the plasma stream in each leg.

Another important issue is that of the accuracy to which one should maintain the magnetic configuration: change in any of the plasma parameters that would break the conditions (2)-(4) will, generally speaking, cause the splitting of the third-order null into three closely spaced first-order nulls, very much like this occurs in the snowflake divertor [1, 2, 6], where an exact second-order null splits into two first-order nulls.

Calculations can be significantly simplified by representing the magnetic field in the complex form, $F(z) = B_x(x,y) + iB_y(x,y)$, with z being a complex coordinate, $z = x + iy$. We denote the complex field by F , not to confuse it with a real vector \mathbf{B}_p . As the magnetic field is both curl-free and divergence-free, one can introduce the complex potential $W(z) = U + iV$ related to F by $F = dW^*/dz$, so that $B_x = -\text{Re}(dW/dz)$, and $B_y = -\text{Im}(dW/dz)$. The Cauchy-Riemann condition for W then yields that $B_x = -\partial V / \partial y$; $B_y = \partial V / \partial x$, so that V is a flux function, see, e.g., [15]. In the complex representation, one has, in particular, instead of Eq. (5):

$$F = iK(2z/a)^3 B_{pm} . \quad (7)$$

The coefficient “ i ” is introduced to have the same orientation of the separatrix branches as in Fig. 2. To be specific, consider the case where the currents in the divertor coils correspond to the set of conditions (3), (4), but the plasma current and its position vary by some small amounts. This situation would mock up a scenario where the control system is set to maintain some constant prescribed currents in the divertor coils, whereas the plasma has some freedom to move.

In the complex representation, the magnetic field of the plasma current is equal to

$$F_p(z) = i(I_p + \delta I_p / 2c)(z - z_0 - \delta z)^{-1} = i(B_{pm} a / 2)(z - z_0 - \delta z)^{-1} , \quad (8)$$

where $z_0=(0, a)$, and $\delta z=(\delta x, \delta y)$. Adding the unperturbed fields of the divertor coils, and making expansion leading to Eq. (7), one finds that around the null-point the field can be described as

$$F(z) = iB_{pm} \left[\frac{1}{2} \left(\frac{\delta z}{ia} + \frac{\delta I_p}{I_p} \right) + K \left(\frac{2z}{a} \right)^3 \right]. \quad (9)$$

The magnetic field nulls are determined from the condition $F(z)=0$. There are three such nulls, forming an equilateral triangle with the center at $z=0$:

$$z_k = \rho \exp i \left(\eta + k \frac{2\pi}{3} \right); \quad k=1,2,3, \quad (10)$$

where

$$\rho = a \left(\frac{1}{16K} \right)^{\frac{1}{3}} \left[\left(\frac{\delta y}{a} - \frac{\delta I_p}{I_p} \right)^2 + \left(\frac{\delta x}{a} \right)^2 \right]^{\frac{1}{6}}. \quad (11)$$

and angle η determines the orientation of the triangle,

$$\eta = \frac{1}{3} \text{Arg} \left[\left(\frac{\delta y}{a} - \frac{\delta I_p}{I_p} \right) + i \frac{\delta x}{a} \right]. \quad (12)$$

The distance from $z=0$ to the nulls, ρ , scales as a cubic root of the deviations of the plasma current and its position from the values to which the divertor currents are tuned to. The presence of this splitting is insignificant as long as we are interested in phenomena occurring at the scales exceeding ρ . As an example, consider the case mentioned after Eq. (6). Substituting the same values of a and K into Eq. (11), we find that ρ is less than 70 cm if the current mismatch is less than 6%. This is well within the capability of the PF control systems.

Of some interest is also a structure of the poloidal magnetic field in the area around the origin, where the three nulls are situated. In particular, we will be interested in the structure of

the separatrices and flux surfaces in this area. We will normalize all the distances around the null by the parameter ρ and will not write any numerical coefficient in front of the expression for the magnetic field, as the shape of the flux surfaces does not depend on this coefficient. So, we use an expression

$$F = i(z - z_1)(z - z_2)(z - z_3) \quad (13)$$

with z_k defined by Eq. (10) with $\rho=1$. The nulls satisfy several simple relations:

$$z_1 + z_2 + z_3 = 0 ; z_1 z_2 + z_1 z_3 + z_2 z_3 = 0 ; z_1 z_2 z_3 = \exp(3i\eta) . \quad (14)$$

Therefore, the function (13) can be re-written as

$$F = i[z^3 - \exp(3i\eta)] . \quad (15)$$

With that, the complex potential becomes

$$W^* = i \left[\frac{z^4}{4} - z \exp(3i\eta) \right] \quad (16)$$

Taking the imaginary part of W^* , one finds the flux function V :

$$V = \frac{x^4 - 6x^2y^2 + y^4}{4} - x \cos(3\eta) - y \sin(3\eta) \quad (17)$$

The condition $V=\text{const}$ determines a certain flux surface. To find the separatrices passing through the null-points of the magnetic field one has to equate expression (17) consecutively to its values at the corresponding null-points of the magnetic field. Using Eq. (15), one finds the following equations for the separatrices:

$$V(x, y) = -\frac{3}{4} \cos\left(4\eta - \frac{2\pi}{3}k\right), \quad (18)$$

where V is defined by Eq. (17). They are shown in Fig. 3a for $\eta=0.2$. This is a typical structure of the separatrices near an “approximate” third-order null. If, however, the distance ρ between the

three nulls is small (i.e. the deviations from an exact clover-leaf configurations are small), then at larger distance from the null we recover 8 branches of the separatrix (Fig. 3b).

In summary: the 3rd-order PF null (generating a “cloverleaf” four-petal structure) can be created by PF coils situated at a significant distance from the null, certainly outside the divertor structure. The potential of this configuration is related to the formation of a large zone of the poloidal field around the null (or a set of closely-spaced first-order nulls). This is very favorable for heat-flux spreading between all six divertor legs and broadening of the plasma flow in each leg [12, 13]. Concerns are related to the control problems, as one would have now to bring together three nulls (not two as in a snowflake). Another problem is related to the possibility to deploy the PF coils outside the toroidal field coils in reactors. Analysis of benefits vs. difficulties will determine the feasibility of this configuration for the existing and future devices.

This work was performed under the auspices of the U.S. Department of Energy by Lawrence Livermore National Security, LLC, Lawrence Livermore National Laboratory, under Contract DE-AC52-07NA27344.

References

1. D.D. Ryutov. Phys. Plasmas, **14**, 064502 (2007).
2. D.D. Ryutov, R.H. Cohen, T.D. Rognlien, M.V. Umansky. Phys. Plasmas, **15**, 092501 (2008)
3. F. Piras, S. Coda, I. Furno, et al. Plasma Phys. Contr. Fusion **51**, 055009 (2009)
4. V. A. Soukhanovskii, J.-W. Ahn, R. E. Bell, et al. Nucl. Fus., **51**, 012001 (2011).
5. S. L. Allen, V. A. Soukhanovskii, T.H. Osborne, et al. “Results From Initial Snowflake Divertor Physics Studies on DIII-D.” Post-deadline paper at 2012 IAEA Fusion Energy Conference, San-Diego, October 8-12, 2012.
6. M.V. Umansky, R.H. Bulmer, R.H. Cohen, et al. Nuclear Fusion, **49**, 075005, 2009.
7. D.D. Ryutov, M.A. Makowski, M.V. Umansky. PPCF, **52**, 105001 (2010).
8. D.D. Ryutov, M.V. Umansky. “Phys. Plasmas,” **17**, 014501 (2010).
9. M. Kotschenreuther, P. M. Valanju, S. M. Mahajan et al., 2004 IAEA Fusion Energy Conference, Vilamoura, Portugal, 1–6 November 2004, International Atomic Energy Agency, Vienna, 2004, paper IC/P6-43.
10. M. Kotschenreuther, P. Valanju, S. Mahajan, and J. Wiley. Phys. Plasmas **14**, 72502 (2007)
11. P.M. Valanju, M. Kotschenreuther, S.M. Mahajan, and J. Canik, Phys. Plasmas **16**, 056110 (2009).
12. D. D. Ryutov, R.H. Cohen , T.D. Rognlien and M. V. Umansky. Contrib. Plasma Phys., **52**, 539 (2012).
13. D. D. Ryutov, R.H. Cohen, T.D. Rognlien and M. V. Umansky. PPCF, **54**, 124050 (2012).
14. K. Lackner and H. Zohm. Fusion Science and Technology” **63**, 43 (2013).
15. J.W. Brown, R. V. Churchill. “*Complex variables and applications*” McGraw Hill, Boston-New York-Toronto, 2004.

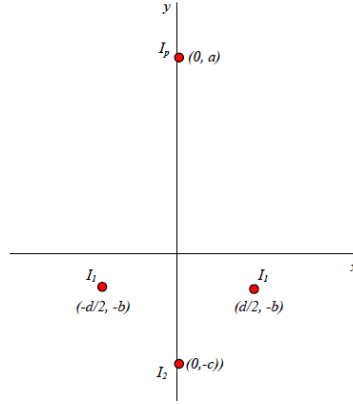


Fig. 1 The four-wire model. The plasma current I_p is at the distance of a from the PF null-point situated at $x=0, y=0$. Two poloidal field coils are situated symmetrically with respect to the vertical axis; one coil lies on the axis. The signs in the brackets representing the coordinates of the currents are chosen to have parameters a, b, c and d positive. The major axis is to the left

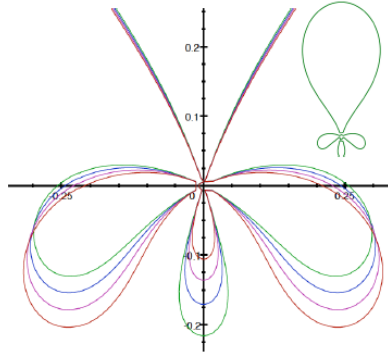


Fig. 2 The structure of the separatrixes near the null-point for $d=0.5a$. The parameter b and the normalized currents are presented in Table 1. If one includes into picture the upper part of the separatrix, it starts looking as a four-petal clover leaf (see inset at the top). So, a more concise name for this configuration could be a “cloverleaf divertor.”

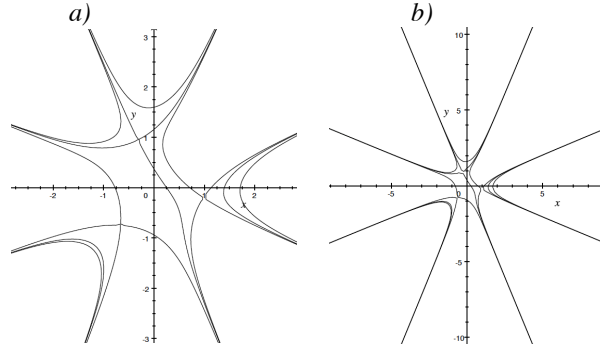


Fig. 3 Structure of separatrices near the origin in the case $\eta=0.2$. The confined plasma is situated in the upper-most zone. The distances are normalized to the parameter ρ , Eq. (11). The panels *a)* and *b)* illustrate the structure of the null region at two “magnifications”: In panel *a)* a close-up view is presented, whereas in panel *b)* a 3-time broader domain is shown. One sees that at larger distances from the origin, the system becomes essentially indistinguishable from an “exact” cloverleaf divertor, with eight branches of the separatrix clearly visible.

Table 1 The parameters of the divertor coils for the cases illustrated by Fig. 3

color	b	c	I_1 (current per conductor)	I_2	K
red	0.14	0.0954	0.2369	0.0183	12.86
purple	0.12	0.1222	0.2197	0.0384	10.62
blue	0.10	0.1522	0.1987	0.0688	8.96
green	0.08	0.1899	0.1747	0.1129	7.54